Portugaliae Electrochimica Acta 2012, 30(6), 405-417

DOI: 10.4152/pea.201206405

PORTUGALIAE ELECTROCHIMICA ACTA
ISSN 1647-1571

A Combined Experimental and Theoretical Study on the Corrosion Inhibition and Adsorption Behaviour of Quinoxaline Derivative During Carbon Steel Corrosion in Hydrochloric Acid

H. Zarrok,[a] A. Zarrouk,[b,*] R. Salghi,[c] H. Oudda,[a] B. Hammouti,[b] M. Ebn, Touhami,[d] M. Bouachrine[e] and S. Boukhris[f]

[a] *Laboratoire des procèdes de séparation, Faculté des Sciences, Université Ibn Tofail BP 242, 14000 Kénitra, Morocco*
[b] *LCAE-URAC18, Faculté des Sciences, Université Mohammed Ier B.P. 717, 60000 Oujda, Morocco*
[c] *Equipe de Génie de l'Environnement et de Biotechnologie, ENSA, Université Ibn Zohr, BP 1136 Agadir, Morocco*
[d] *Laboratoire d'électrochimie, de corrosion et d'environnement, Faculté des Sciences, Université Ibn Tofail BP 242, 14000 Kenitra, Morocco*
[e] *ESTM, University Moulay Ismail, BP 3130, Toulal, Meknès, Morocco*
[f] *Equipe de Synthèse Organique, Organométallique et d'Agrochimie, Faculté des Sciences, Université Ibn Tofail, B.P. 133, 14000 Keénitra, Morocco*

Received 23 November 2012; accepted 23 December 2012

Abstract

The corrosion inhibitive effects of 2-(4-methylphenyl)-1,4-dihydroquinoxaline (Q1) on carbon steel surface in hydrochloric acid solution was studied using weight loss measurements, electrochemical impedance spectroscopy (EIS), Tafel polarization techniques and quantum chemical approach, using the density functional theory (DFT). Inhibition efficiency increased with increase in concentration of the inhibitor. The degree of surface coverage of the adsorbed inhibitor was determined by weight loss technique, and it was found that the results obeyed Langmuir adsorption isotherm. Tafel polarization data indicated that this inhibitor is of mixed type. EIS shows that charge-transfer resistance increases and the capacitance of double layer decreases with the inhibitor concentration, confirming the adsorption process mechanism. Trends in the calculated molecular properties (e.g., dipole moment, HOMO and LUMO energies) were compared with trends in the experimentally determined inhibition efficiency. The results show that trends in the quantum chemical descriptors are in agreement with the experimentally determined inhibition efficiencies.

***Keywords**:* quinoxaline, steel, corrosion inhibition, electrochemical techniques, DFT.

[*] Corresponding author. E-mail: azarrouk@gmail.com

Introduction

Hydrochloric acid is generally used in industry as chemical cleaning, oil well cleaning, descaling, and pickling for the removal of undesirable scale and rust from the metallic surfaces. The corrosion of steel is an important concern that has received a considerable amount of attention [1-4]. Using inhibitors is an important method of protecting materials against acid attack, reducing the metal dissolution and the consumption of acid. The efficiency of an organic compound as an inhibitor is mainly dependent on its ability to get adsorbed on metal. These inhibitors contain oxygen, nitrogen, sulfur heteroatoms, and multiple bonds. This phenomenon is influenced by the nature and surface charge of the metallic surface, testing media, and chemical structure of inhibitors [5-22]. Investigating and exploring new corrosion inhibitor for steel corrosion in acid solutions are important for its practical application.

Quinoxaline derivatives as important N-heterocyclic compounds are easy to synthesize and readily available. Their ring moiety constitutes part of the chemical structures of various antibiotics such as echinomycin, levomycin and actinoleucin [23,24]. Abboud et al. [25] have studied the inhibition effect of 2,3-quinoxalinedione on the corrosion of mild steel in 1.0 M HCl solution. More recently [18], we have reported on the effectiveness of 2-(4-methylphenyl)-1,4-dihydroquinoxaline as inhibitor of copper corrosion in 2.0 M HNO_3. The results obtained for the two studies showed that quinoxaline derivatives are excellent inhibitors for copper and steel in acidic media. In continuation of our study on quinoxaline derivatives as inhibitors of carbon steel corrosion in acidic media, we report the inhibitive properties of 2-(4-methylphenyl)-1,4-dihydroquinoxaline as carbon steel corrosion inhibitor in 1.0 M HCl using weight loss technique, potentiokinetic polarization methods, electrochemical impedance spectroscopy (EIS) and quantum chemical calculations. The choice of this compound was based on the consideration that it contains many π-electrons and two N atoms which induce greater adsorption of the inhibitor compared with compounds containing only one N atom. The chemical structure of the studied quinoxaline derivative is given in Fig. 1.

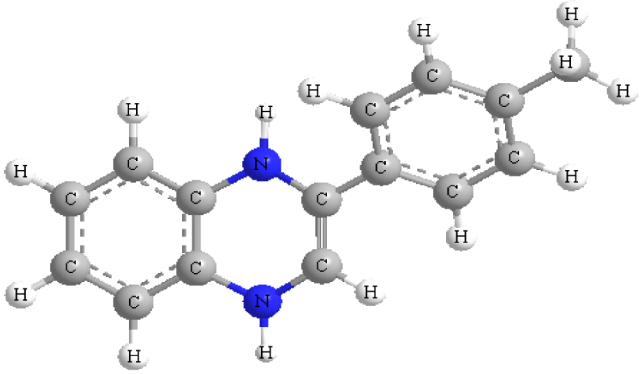

Figure 1. Chemical structure of the studied quinoxaline compound.

Experimental method

Materials

The steel used in this study is a carbon steel (CS) (Euronorm: C35E carbon steel and US specification: SAE 1035) with a chemical composition (in wt%) of 0.370 % C, 0.230 % Si, 0.680 % Mn, 0.016 % S, 0.077 % Cr, 0.011 % Ti, 0.059 % Ni, 0.009 % Co, 0.160 % Cu and the rest being iron (Fe).

Solutions

The aggressive solutions of 1.0 M HCl were prepared by dilution of analytical grade 37% HCl with distilled water. The concentration range of 2-(4-methylphenyl)-1,4-dihydroquinoxaline (Q1) used was 10^{-6} M to 10^{-3} M.

Weight loss measurements

The carbon steel (CS) sheets of 1.6 × 1.6 × 0.07 cm were abraded with a series of emery papers SiC (120, 600 and 1200) and then washed with distilled water and acetone. After weighing accurately, the specimens were immersed in an 80 mL beaker containing 50 mL 1.0 M HCl solution with and without addition of different concentrations of Q1. All the aggressive acid solutions were open to air. After 6 h the specimens were taken out, washed, dried, and weighed accurately. In order to get good reproducibility experiments were carried out in triplicate. The average weight loss of three parallel CS sheets was obtained. The tests were repeated at 308 K. The corrosion rate (ν) and the inhibition efficiency (η_{WL}) were calculated by the following equations [26]:

$$\nu = \frac{W}{St} \times 100 \quad (1)$$

$$\eta_{WL}(\%) = \frac{\nu_0 - \nu}{\nu_0} \times 100 \quad (2)$$

where W is the three-experiment average weight loss of the carbon steel, S is the total surface area of the specimen, t is the immersion time and ν_0 and ν are values of the corrosion rate without and with addition of the inhibitor, respectively.

Electrochemical impedance spectroscopy

The electrochemical measurements were carried out using a Volta lab (Tacussel-Radiometer PGZ 100) potentiostate and controlled by Tacussel corrosion analysis software model (Voltamaster 4) at under static condition. The corrosion cell used had three electrodes. The reference electrode was a saturated calomel electrode (SCE). A platinum electrode was used as auxiliary electrode of surface area of 1 cm^2. The working electrode was carbon steel. All potentials given in this study were referred to this reference electrode. The working electrode was immersed in test solution for 30 minutes to a establish steady state open circuit potential (*E*ocp). After measuring the *E*ocp, the electrochemical measurements were performed. All electrochemical tests have been performed in aerated solutions at 308 K. The EIS experiments were conducted in the frequency range with high limit of 100 kHz and different low limit 0.1 Hz at open circuit potential, with 10 points per decade, at the rest potential, after 30 min of acid

immersion, by applying 10 mV ac voltage peak-to-peak. Nyquist plots were made from these experiments. The best semicircle can be fit through the data points in the Nyquist plot using a non-linear least square fit so as to give the intersections with the *x*-axis.
The inhibition efficiency of the inhibitor was calculated from the charge transfer resistance values using the following equation [27]:

$$\eta_z\% = \frac{R_{ct}^{i} - R_{ct}^{\circ}}{R_{ct}^{i}} \times 100 \qquad (3)$$

where, R_{ct}° and R_{ct}^{i} are the charge transfer resistance in absence and in presence of inhibitor, respectively.

Potentiodynamic polarization
The electrochemical behaviour of carbon steel sample in inhibited and uninhibited solution was studied by recording anodic and cathodic potentiodynamic polarization curves. Measurements were performed in the 1.0 M HCl solution containing different concentrations of the tested inhibitor by changing the electrode potential automatically from -800 to -100 mV versus corrosion potential at a scan rate of 1 mV s^{-1}. The linear Tafel segments of anodic and cathodic curves were extrapolated to corrosion potential to obtain corrosion current densities (I_{corr}). From the polarization curves obtained, the corrosion current (I_{corr}) was calculated by curve fitting using the equation:

$$I = I_{corr}\left[exp\left(\frac{2.3\Delta E}{\beta_a}\right) - exp\left(\frac{2.3\Delta E}{\beta_c}\right)\right] \qquad (4)$$

The inhibition efficiency was evaluated from the measured I_{corr} values using the relationship:

$$\eta_{Tafel}\% = \frac{I_{corr}^{\circ} - I_{corr}^{i}}{I_{corr}^{\circ}} \times 100 \qquad (5)$$

where, I_{corr}° and I_{corr}^{i} are the corrosion current density in absence and presence of inhibitor, respectively.

Quantum chemical calculations
All theoretical calculations were performed using DFT (density functional theory) with the Beck's three parameter exchange functional along with the Lee-Yang-Parr nonlocal correlation functional (B3LYP) [28-30] with 6- 31G* basis set is implemented in Gaussian 03 program package [31]. This approach is shown to yield favorable geometries for a wide variety of systems. The following quantum chemical parameters were calculated from the obtained optimized molecular structure: the energy of the highest occupied molecular orbital (E_{HOMO}), the energy of the lowest unoccupied molecular orbital (E_{LUMO}), the

energy band gap ($\Delta E_{gap} = E_{HOMO} - E_{LUMO}$), the dipole moment ($\mu$) and total energy (*TE*).

Results and discussion

Electrochemical impedance spectroscopy

Nyquist plots for carbon steel in 1.0 M HCl solution in the absence and presence of the inhibitor at various concentrations (at 308 K) are shown in Fig. 2. The semicircle Nyquist plots can be modeled by a simple "Randles" circuit, including the "charge-transfer resistance" (R_{ct}) parallel with the double layer capacitance (C_{dl}) in series with the solution resistance (R_s). As shown in Fig. 2, the Nyquist plots for carbon steel in 1.0 M HCl for the inhibitor were not perfect semicircles. This difference can be explained by the non-ideal behavior of the double layer as a capacitor. Therefore, it is necessary to use a constant phase element (CPE) instead of the double layer capacity to account for non-ideal behavior.

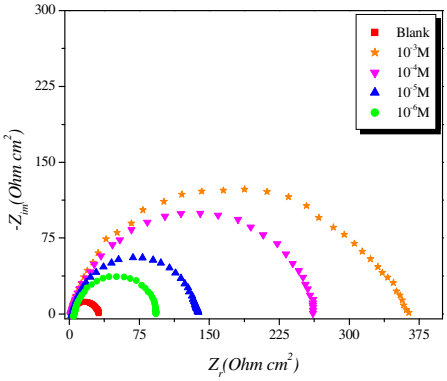

Figure 2. Nyquist diagrams for carbon steel in 1.0 M HCl containing different concentrations of Q1 at 308 K.

The appearance of the CPE element is often related to the electrode roughness or to the inhomogeneity in the conductance or dielectric constant [32,33]. The CPE can be modeled as follows [34]:

$$Z_{CPE} = A^{-1} (i\,\omega)^{-n} \qquad (6)$$

here A is the CPE constant (in Ω^{-1} S^n cm^{-2}), ω is the sine wave modulation angular frequency (in rad s^{-1}), $i^2 = -1$ is an imaginary number, and n is an empirical exponent ($0 \leq n \leq 1$) which measures the deviation from the ideal capacitive bahaviour [35]. The quantitative results of impedance measurements (calculated by Zview program) for the Q1 are given in Table 1.

For the appraisal of the experimental Nyquist plots, equivalent circuit models, which physically correctly represent the systems under investigation, must be applied. The simplest model consists of the solution resistance (R_s) in series with the parallel combination of the constant phase element (CPE) in place of the double-layer capacitance (C_{dl}), and charge-transfer resistance (R_{ct}) was used.

Such equivalent circuit (Fig. 3) has been used previously to model the carbon steel/acid interface [36].

Table 1. Impedance parameters for corrosion of steel in 1.0 M HCl in the absence and presence of different concentrations of Q1 at 308 K.

Conc (M)	R_s (Ω cm^2)	R_{ct} (Ω cm^2)	n	A×10^{-4} (s^n Ω^{-1}cm^{-2})	C_{dl} (μF cm^{-2})	η_z (%)
Blank	1.67	29.66	0.91	0.146120	85.31	-----
10^{-3}	1.76	328.00	0.85	0.078687	27.49	91.0
10^{-4}	2.18	250.50	0.87	0.080232	31.73	88.2
10^{-5}	3.44	129.90	0.89	0.095215	41.62	77.2
10^{-6}	5.53	086.00	0.91	0.105190	52.60	65.5

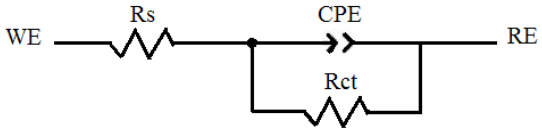

Figure 3. The electrochemical equivalent circuit used to fit the impedance measurements.

Inspection of the data in Fig. 2 and Table 1 reveals that the corrosion of carbon steel was decreased in the presence of the inhibitor because the charge-transfer resistance of carbon steel was significantly increased. Table 1 shows that the addition of the quinoxaline into the corrosive solution caused an increase in the inhibition efficiency and in the charge-transfer resistance, and a decrease in the double-layer capacitance (C_{dl}) given as [37]

$$C_{dl} = \frac{\varepsilon \varepsilon_0 A}{d} \qquad (7)$$

where ε_0 is the vacuum dielectric constant, ε is the local dielectric constant, d is the thickness of the double layer, and A is the surface area of the electrode. According to Eq. 3, a decrease in C_{dl} can happen if the inhibitor molecules (low dielectric constant) replace the adsorbed water molecules (high dielectric constant) on the carbon steel surface. The capacitance is inversely proportional to the thickness of the double layer. Thus, decrease in the C_{dl} values could be attributed to the adsorption of Q1 on the metal surface. Decrease in the capacitance, which can result from a decrease in the local dielectric constant and/or an increase in the thickness of the electrical double layer, strongly suggests that the inhibitor molecules adsorbed at the metal / solution interface. In the absence and in the presence of inhibitor, phase-shift value remains more or less identical; this indicates that the charge-transfer process controls the dissolution mechanism [38] of carbon steel in 1.0 M HCl solution.

In acidic solutions, it is known that inhibitor molecules can be protonated. Thus, in solution, both neutral molecule and cationic forms of inhibitor exist [39]. It is assumed that Cl^- ion is first adsorbed onto the positively charged metal surface

by coulombic attraction and then inhibitor molecules can be absorbed through electrostatic interactions between the positively charged molecules and the negatively charged metal surface [39]. These adsorbed molecules interact with $(FeCl^-)_{ads}$ species to form monomolecular layers (by forming a complex) on the steel surface. These layers protect the carbon steel surface from attack by chloride ions. Thus, the oxidation of $(FeCl^-)_{ads}$ into Fe^{++} can be prevented. On the other hand, the protonated inhibitor molecules are also adsorbed at cathodic sites in competition with hydrogen ions reducing hydrogen evolution. Inhibition performance of Q1 for carbon steel/ 1.0 M HCl interface depends on several factors such as the number of adsorption sites, molecular size, mode of interaction with the metal surface, and extent of formation of metallic complexes [40]. The adsorption of Q1 at the carbon steel surface can take place through its two nitrogen polar atoms in addition to π-electron interaction of the benzene rings with unshared d electrons of iron atoms.

Potentiodynamic polarization study

Fig. 4 shows the influence of Q1 concentration on the cathodic and anodic potentiodynamic polarization curves of steel in 1.0 M HCl. Electrochemical corrosion parameters such as corrosion potential (E_{corr}), cathodic Tafel slops (β_c), corrosion current density (I_{corr}) and the inhibition efficiency values are collected in Table 2. Figure 4 and Table 2 show that the I_{corr} values decrease considerably with the increase of Q1 concentration. No definite trend was observed in the shift of E_{corr} values, in the presence of various concentrations of this inhibitor, in acidic media. The presence of the inhibitor lowers the cathodic Tafel slope values probably by blocking the metal surface. For potentials higher than -420 mV vs. SCE, the presence of Q1 did not change the current vs. the potential. This potential can be defined as the desorption potential. For the inhibited system, if the displacement in E_{corr} value is greater than 85 mV relative to the uninhibited system, then the inhibitor is classified as cathodic or anodic type [41, 42]. In our case, the maximum displacement of E_{corr} value is 37.4 mV, hence the 2-(4-methylphenyl)-1,4-dihydroquinoxaline is classified as a mixed-type inhibitor.

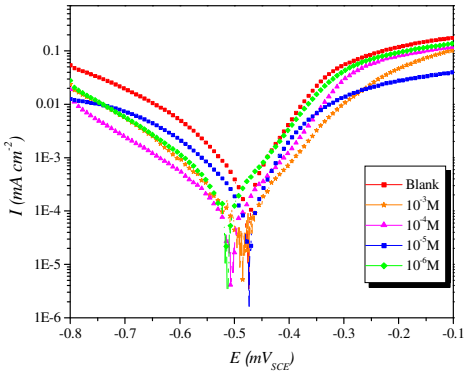

Figure 4. Polarisation curves of carbon steel in 1.0 M HCl for various concentrations of Q1.

Table 2. Polarization data of carbon steel in 1.0 M HCl without and with addition of inhibitor at 308 K.

Inhibitor	Conc (M)	$-E_{corr}$ (mV/SCE)	$-\beta_c$ (mV dec^{-1})	I_{corr} (μA cm^{-2})	η_{Tafel} (%)
HCl	1	475.9	176.0	1077.8	-
Q1	10^{-3}	485.2	102.0	95.3	91.1
	10^{-4}	506.3	168.5	124.0	88.5
	10^{-5}	474.5	169.5	243.9	77.4
	10^{-6}	513.3	153.9	350.1	67.5

Weight loss measurements

Table 3 gives the values of inhibition efficiency obtained from the weight loss measurements for different concentrations of Q1 in 1.0 M HCl at 308 K after 6 h immersion. The inhibition efficiency increases with increasing the inhibitor concentration. The optimum concentration required to achieve an efficiency of 94.2% was found to be 10^{-3} M. The inhibition by Q1 can be explained in terms of adsorption on the metal surface. The compound can be adsorbed by the interaction between the lone pair of electrons of the nitrogen atom of the quinoxaline and the metal surface. This process is facilitated by the presence of π vacant orbitals of low energy in the iron atom, as observed in transition group metals. Moreover, the formation of positively charged protonated Q1 species in acidic solutions facilitates the adsorption of the compound on the metal surface through electrostatic interactions between the organic molecules and the metal surface.

Table 3. Corrosion parameters obtained from weight loss measurements for carbon steel in 1.0 M HCl containing various concentration of inhibitor at 308 K.

Inhibitor	Conc (M)	ν (mg/cm^2 h)	η_{WL} (%)	θ
Blank	1	1.070	-----	-----
Q1	1×10^{-3}	0.062	94.2	0.942
	1×10^{-4}	0.106	90.1	0.901
	1×10^{-5}	0.211	80.3	0.803
	1×10^{-6}	0.340	68.2	0.682

Adsorption isotherm and thermodynamic parameters

It is well established that the first step in corrosion inhibition of metals and alloys is the adsorption of organic inhibitor molecules at the metal/solution interface and that the adsorption depends on the molecule's chemical composition, the temperature and the electrochemical potential at the metal/solution interface. In fact, the solvent water molecules could also adsorb at metal/solution interface. So the adsorption of organic inhibitor molecules from the aqueous solution can be regarded as a quasi-substitution process between the organic compounds in the aqueous phase [$Org_{(sol)}$] and water molecules at the electrode surface [$H_2O_{(ads)}$] [43]

$$Org_{aq} + xH_2O_{ads} \leftrightarrow xH_2O_{aq} + Org_{ads} \qquad (8)$$

where x, the size ratio, is the number of water molecules displaced by one molecule of organic inhibitor. x is assumed to be independent of coverage or charge on the electrode [44].

Basic information on the interaction between the inhibitor and the alloy surface can be provided by the adsorption isotherm. In order to obtain the isotherm, the fractional coverage values θ as a function of inhibitor concentration (C_{inh}) must be obtained. It is well known that θ can be obtained from the $\eta_{WL}\%/100$ ratio. Attempts were made to fit the θ values to various isotherms, including Langmuir, Temkin, Frumkin and Flory-Huggins. Many adsorption isotherms were plotted and the Langmuir adsorption isotherm was found to be the best description of the adsorption behavior of the studied inhibitors. According to this isotherm, θ is related to equilibrium adsorption constant (K_{ads}) and C_{inh} by the relation

$$\frac{C_{\text{inh}}}{\theta} = \frac{1}{K_{\text{ads}}} + C_{\text{inh}} \qquad (9)$$

Fig. 5 shows the plot of C_{inh}/θ vs. C_{inh} and the expected linear relationship is obtained. The value of the regression coefficient (R^2) confirmed the validity of this approach. The slope of this straight line is 1.06, suggesting that adsorbed inhibitor molecules form monolayer on the carbon steel surface and that there is no interaction among the adsorbed inhibitor molecules. On the other hand, the equilibrium constant of adsorption is related to the standard energy of adsorption (ΔG°_{ads}) by the relation [45]

$$K_{ads} = (\frac{1}{55.5})\exp(-\frac{\Delta G^{\circ}_{ads}}{RT}) \qquad (10)$$

where R is the gas constant, T is the absolute temperature of experiment, and the constant value of 55.5 is the concentration of water in solution in mol L^{-1} [46].

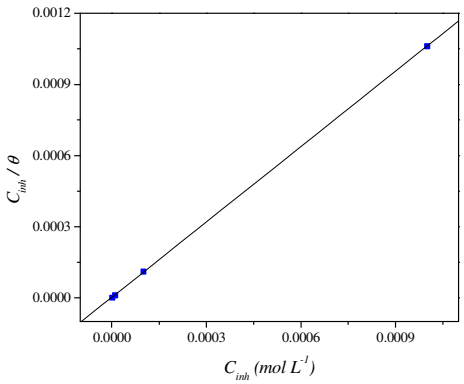

Figure 5. Langmuir adsorption of Q1 on the carbon steel surface in 1.0 HCl solution.

The values of thermodynamic parameters are listed in Table 4. The values of K_{ads} and ΔG°_{ads} increase with increasing the inhibitor concentration, suggesting stronger interaction between the inhibitor molecules and the iron surface atoms. The high value of these parameters indicates that stronger and more stable adsorbed layer is formed at carbon steel/acid solution interface, which results in the higher inhibition efficiency [47]. Furthermore, the values of ΔG°_{ads} for the

quinoxaline compound is negative (Table 4) and this value is consistent with the spontaneity of the adsorption process and the stability of the adsorbed layer on the carbon steel surface [48]. Generally, ΔG°_{ads} values of -20 kJ mol^{-1} or higher are associated with an electrostatic interaction between charged molecules and charged metal surface (physisorption); those of -40 kJ mol^{-1} or lower involve charge sharing or transfer from the inhibitor molecules to the metal surface to form a coordinate covalent bond, (chemisorption) [49]. ΔG°_{ads} is equal to -43.02 kJ mol^{-1}; this high value shows that in the presence of 1.0 M HCl chemisorption of Q1 may occur.

Table 4. Thermodynamic parameters for the adsorption of Q1 in 1.0 M HCl on the carbon steel at 308 K.

Inhibitor	Slope	K_{ads} (M^{-1})	R^2	ΔG°_{ads} (kJ/mol)
Q1	1.06	426012.31	0.99999	-43.48

Theoretical calculations

The major thrust of quantum chemical research is to understand and explain the functions of these heterocyclic compounds in molecular terms. In order to support experimental data, theoretical calculations were conducted in order to provide molecular-level understanding of the observed experimental behaviour. Among quantum chemical methods for evaluation of corrosion inhibitors, DFT has shown significant promise [50] and appears to be adequate for pointing out the changes in the electronic structure responsible for the inhibitory action. In recent years, a hybrid version of DFT/HF methods, i.e., B3LYP has been applied successfully to model systems containing transition metal atoms [51]. Briefly, this method uses a Becke's three parameter functional (B3) and includes a mixture of HF with DFT exchange terms associated with the gradient corrected correlation functional of Lee, Yang and Parr (LYP) [30]. The molecular structure in the most stable conformation found was optimized and the HOMO and the LUMO energies calculated employing B3LYP functional with the 6-31g(d) basis set. The optimized structures are shown in Fig. 6. From Fig. 7, it can be observed that both HOMO and LUMO are mainly distributed on the area of the quinoxaline and phenol ring in the studied compound, indicating that these rings are main adsorption centers of the quinoxaline derivative.

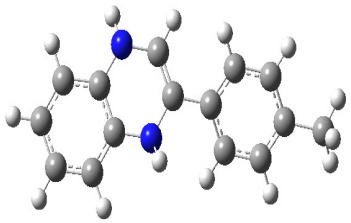

Figure 6. Optimized molecular structure of Q1 by B3LYP-6-31 G(d) method.

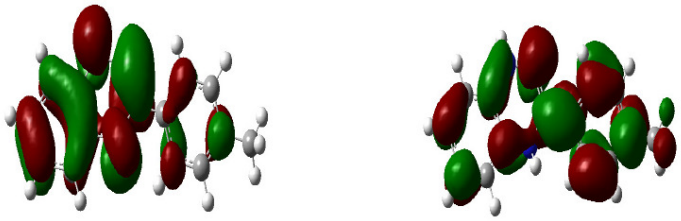

Figure 7. The frontier molecule orbital density distributions of Q1: HOMO (left); LUMO (right).

Table 5. The calculated quantum chemical parameters of Q1.

Compound	TE (eV)	E_{HOMO} (eV)	E_{LUMO} (eV)	ΔE_{gap} (eV)	μ (Debye)
Q1	-689.5219132	-4.0708	-0.5269	3.543	0.9198

Table 5 shows some of the key quantum chemical parameters computed using DFT method. These are mainly the energies of the highest occupied (E_{HOMO}) and lowest unoccupied (E_{LUMO}) molecular orbitals, energy of the gap, ΔE (E_{LUMO} - E_{HOMO}) and dipole moment (μ). These quantum chemical parameters were obtained after geometric optimization with respect to all nuclear coordinates. It has been reported that E_{HOMO} is often associated with the electron donating ability of a molecule, whereas E_{LUMO} indicates its ability to accept electrons. The high values of E_{HOMO} (-4.0708 eV) are likely to indicate a tendency of the molecule to donate electrons to appropriate acceptor molecules with low energy and empty molecular orbital, whereas the value of E_{LUMO} (-0.5269 eV) indicates its ability of the molecule to accept electrons. Consequently, the value of ΔE_{gap} provides a measure for the stability of the formed complex on the metal surface. The total energy of the quinoxaline is equal to -689.5219132 eV. This result indicated that quinoxaline is favourably adsorbed through the active centers of adsorption. Lower values of dipole moment (μ) will favour accumulation of the inhibitor in the surface layer and therefore higher inhibition efficiency [52].

Conclusions

2-(4-methylphenyl)-1,4-dihydroquinoxaline is a good inhibitor (94.2% inhibition efficiency observed at 10^{-3} M) for carbon steel in 1.0 M HCl.

Polarization curves indicated that Q1 is a mixed-type inhibitor. The inhibition efficiencies obtained from polarization and EIS were in good agreement.

The adsorption of inhibitor molecules on the carbon steel surface in 1.0 M HCl solution followed Langmuir adsorption isotherm.

The values obtained for ΔG°_{ads} showed chemisorption.

The calculated quantum chemical parameters such as HOMO-LUMO gap (ΔE_{L-H}), E_{HOMO}, E_{LUMO}, dipole moment (μ) and total energy (TE) were found to give reasonably good correlation with the efficiency of the corrosion inhibition.

References

1. Singh AK, Chaudhary V, Sharma A. Port Electrochim Acta. 2012;30:99.
2. Prajila M, Sam J, Bincy J, Abraham J. J Mater Environ Sci. 2012;3:1045.
3. Naik UJ, Panchal VA, Patel AS, Shah NK. J Mater Environ Sci. 2012;3:935.
4. Zarrouk A, Zarrok H, Salghi R, Hammouti B, Bentiss F, Touir R, Bouachrine M. J Mater Environ Sci. 2013;4: 177.
5. Zarrok H, Oudda H, Zarrouk A, Salghi R, Hammouti B, Bouachrine M. Der Pharm Chem. 2011;3:576.
6. Zarrok H, Salghi R, Zarrouk A, Hammouti B, Oudda H, Bazzi Lh, Bammou L, Al-Deyab SS. Der Pharm Chem. 2012;4:407.
7. Zarrok H, Al-Deyab SS, Zarrouk A, Salghi R, Hammouti B, Oudda H, Bouachrine M, Bentiss F. Int J Electrochem Sci. 2012;7:4047.
8. Hmamou DB, Salghi R, Zarrouk A, Zarrok H, Hammouti B, Al-Deyab SS, Bouachrine M, Chakir A, Zougagh M. Int J Electrochem Sci. 2012;7:5716.
9. Zarrouk A, Hammouti B, Al-Deyab SS, Salghi R, Zarrok H, Jama C, Bentiss F. Int J Electrochem Sci. 2012;7:5997.
10. Zarrouk A, Zarrok H, Salghi R, Hammouti B, Al-Deyab SS, Touzani R, Bouachrine M, Warad I, Hadda TB. Int J Electrochem Sci. 2012;7:6353.
11. Zarrouk A, Messali M, Zarrok H, Salghi R, Al-Sheikh Ali A, Hammouti B, Al-Deyab SS, Bentiss F. Int J Electrochem Sci. 2012;7:6998.
12. Zarrok H, Zarrouk A, Salghi R, Ramli Y, Hammouti B, Al-Deyab SS, Essassi EM, Oudda H. Int J Electrochem Sci. 2012;7:8958.
13. Hmamou DB, Salghi R, Zarrouk A, Zarrok H, Al-Deyab SS, Benali, Hammouti O, B. Int J Electrochem Sci. 2012;7:8988.
14. Zarrouk A, Messali M, Aouad MR, Assouag M, Zarrok H, Salghi R, Hammouti B, Chetouani A. J Chem Pharm Res. 2012;4:3427.
15. Hmamou DB, Aouad MR, Salghi R, Zarrouk A, Assouag M, Benali O, Messali M, Zarrok H, Hammouti B. J Chem Pharm Res. 2012;4:3489.
16. Zarrok H, Oudda H, El Midaoui A, Zarrouk A, Hammouti B, Ebn Touhami M, Attayibat A, Radi S, Touzani R. Res Chem Intermed. In press. DOI: 10.1007/s11164-012-0525-x
17. Zarrouk A, Hammouti B, Zarrok H, Salghi R, Dafali A, Bazzi Lh, Bammou L, Al-Deyab SS. Der Pharm Chem. 2012;4:337.
18. Zarrouk A, Dafali A, Hammouti B, Zarrok H, Boukhris S, Zertoubi M. Int J Electrochem Sci. 2010;5:46.
19. Zarrouk A, T. Chelfi, A. Dafali, Hammouti B, Al-Deyab SS, I. Warad, N. Benchat, M. Zertoubi, Int. J. Electrochem. Sci. 5 (2010) 696.
20. Zarrouk A, Warad I, Hammouti B, Dafali A, Al-Deyab SS, Benchat N. Int J Electrochem Sci. 2010;5:1516.
21. Zarrouk A, Hammouti B, Touzani R, Al-Deyab SS, Zertoubi M, Dafali A, Elkadiri S. Int J Electrochem Sci. 2011;6:4939.
22. Zarrouk A, Hammouti B, Zarrok H, Al-Deyab SS, Messali M. Int J Electrochem Sci. 2011;6:6261.
23. Dell A, William DH, Morris HR, Smith GA, Feeney J, Roberts GCK. J Am Chem Soc. 1975;97:2497.
24. Bailly C, Echepare S, Gago F, Waring MJ. J Anticancer Drug Des. 1999;15:291.
25. Abboud Y, Abourriche A, Saffaj T, Berrada M, Charrouf M, Bennamara A, Al-Himidi N, Hannache H. Mater Chem Phys. 2007;105:1.
26. Li XH, Deng SD, Fu H, Mu GN, Zhao N. Appl Surf Sci. 2008;254:5574.

27. Zarrok H, Zarrouk A, Hammouti B, Salghi R, Jama C, Bentiss F. Corros Sci. 2012;64:243.
28. Becke AD. J Chem Phys. 1992;96:9489.
29. Becke AD. J Chem Phys. 1993;98:1372.
30. Lee C, Yang W, Parr RG. Phys Rev B. 1988;37:785.
31. Gaussian 03, Revision B.01, Frisch MJ et al. Gaussian, Inc., Pittsburgh, PA; 2003.
32. Avci G. Colloids Surf A. 2008;317:730.
33. Rammelt U, Koehler S, Reinhard G. Corros Sci. 2008;50:1659.
34. Bentiss F, Traisnel M, Gengembre L, Lagrenée M. Appl Surf Sci. 1999;152:237.
35. Macdonald R, Franceschetti DR. In: Impedance spectroscopy. Macdonald JR, editor. New York: Wiley; 1987. P. 96.
36. Growcock FB, Jasinski JH. J Electrochem Soc. 1989;136:2310.
37. Oguzie EE, Li Y, Wang FH. Electrochim Acta. 2007;53:909.
38. Hermas AA, Morad MS, Wahdan MH. J Appl Electrochem. 2004;34:95.
39. Quraishi MA, Rafiquee MZA, Khan S, Saxena N. J Appl Electrochem. 2007;37:1153.
40. Bentiss F, Bouanis M, Mernari B, Traisnel M, Vezin H, Lagrenee M. Appl Surf Sci. 2007;253:3696.
41. Musa AY, Kadhum AAH, Mohamad AB, Takriff MS. Corros Sci. 2010;52:3331.
42. Zhang J, Gong XL, Yu HH, Du M. Corros Sci. 2011;53:3324.
43. Sahin M, Bilgic S, Yilmaz H. Appl Surf Sci. 2002;195:1.
44. Migahed MA, Farag AA, Elsaed SM, Kamal R, Mostfa M, Abd El-Bary H. Mater Chem Phys. 2011;125:125.
45. Kaminski M, Szklarska-Smialowska Z. Corros Sci. 1973;13:557.
46. Olivares O, Likhanova NV, Gomez B, Navarrete J, Llanos-Serrano ME, Arce E, Hallen JM. Appl Surf Sci. 2006;252:2894.
47. Hammouti B, Zarrouk A, Al-Deyab SS, Warad I. Orient J Chem. 2011;27:23.
48. Fouda AS, Heakal FE, Radwan MS. J Appl Electrochem. 2009;39:391.
49. Hosseini M, Mertens SFL, Arshadi MR. Corros Sci. 2003;45:1473.
50. Lopez N, Illas F. J Phys Chem B. 1998;102:1430.
51. Ignaczak A, Gomes JANF. Chem Phys Lett. 1996;257:609.
52. Khalil N. Electrochim Acta. 2003;48:2635.